nature immunology

The proteolytic activity of the paracaspase MALT1 is key in T cell activation

Fabien Rebeaud[1,4], Stephan Hailfinger[1,4], Anita Posevitz-Fejfar[1], Myriam Tapernoux[1], Roger Moser[1], Daniel Rueda[1], Olivier Gaide[1,3], Montserrat Guzzardi[1], Emanuela M Iancu[2], Nathalie Rufer[2], Nicolas Fasel[1] & Margot Thome[1]

The paracaspase MALT1 is pivotal in antigen receptor–mediated lymphocyte activation and lymphomagenesis. MALT1 contains a caspase-like domain, but it is unknown whether this domain is proteolytically active. Here we report that MALT1 had arginine-directed proteolytic activity that was activated after T cell stimulation, and we identify the signaling protein Bcl-10 as a MALT1 substrate. Processing of Bcl-10 after Arg228 was required for T cell receptor–induced cell adhesion to fibronectin. In contrast, MALT1 activity but not Bcl-10 cleavage was essential for optimal activation of transcription factor NF-κB and production of interleukin 2. Thus, the proteolytic activity of MALT1 is central to T cell activation, which suggests a possible target for the development of immunomodulatory or anticancer drugs.

Bcl-10 and MALT1 are signaling proteins that are key in antigen receptor–mediated lymphocyte activation and lymphomagenesis[1–3]. The best characterized function of Bcl-10 and MALT1 is activation of the transcription factor NF-κB, which controls many aspects of leukocyte responses. The NF-κB-activating function of Bcl-10 and MALT1 has been studied most intensively in the context of lymphocyte activation through the antigen receptor. Antigen receptor triggering leads to the activation of receptor-proximal tyrosine kinases that control the phosphorylation and assembly of various adaptor and scaffolding proteins; such proteins then form signaling complexes that enable the recruitment and activation of phospholipase C-γ. Cleavage of phosphatidylinositol-3,4-bisphosphate mediated by phospholipase C-γ then leads to the formation of inositol-3,4,5-trisphosphate, which induces an increase in intracellular calcium and the formation of diacylglycerol, which is essential in activating protein kinase C-β (PKC-β) and PKC-θ in B cells and T cells, respectively. These lymphocyte-specific PKC isoforms can directly phosphorylate the membrane-associated guanylate kinase CARMA1 (also called CARD11 or Bimp3) to induce a conformational change in CARMA1 that allows the formation of a signaling complex containing CARMA1, Bcl-10 and MALT1, together with additional signaling compounds that orchestrate NF-κB activation meditated by inhibitor of NF-κB (IκB) kinase (IKK)[1,2,4,5].

In the CARMA1–Bcl-10–MALT1 signaling complex, Bcl-10 acts as an adaptor protein that binds, through its caspase-recruitment domain (CARD), to the CARD motif of CARMA1 (refs. 6–12); this interaction leads to the recruitment of MALT1 and/or the stabilization of the MALT1-CARMA1 interaction[13–15]. The formation of the CARMA1–Bcl-10–MALT1 complex is central to antigen receptor–mediated activation of the NF-κB pathway and thereby controls the antigen receptor–induced expression and secretion of cytokines that are essential for lymphocyte proliferation[1–3]. It is thought that the association of Bcl-10 and MALT1 with either of the CARMA1-homologous proteins CARMA3 (also called CARD10 or Bimp1) or CARD9 similarly controls NF-κB activation by G protein–coupled receptors or by the zymosan receptor dectin-1, respectively[16]. Collectively, such studies suggest that Bcl-10 and MALT1 function together 'downstream' of various immune and nonimmune receptors to synergistically activate NF-κB-dependent gene transcription.

Despite such progress in understanding the functions of Bcl-10 and MALT1, the exact nature of the physical and functional interaction of Bcl-10 with MALT1 and its molecular consequences for 'downstream' signaling events are not precisely understood. It is thought that Bcl-10-dependent formation of MALT1 oligomers is critical for activation of the IKK complex[17,18], most likely by MALT1-dependent recruitment of the ubiquitin ligase TRAF6 (refs. 17,19) and subsequent lysine 63–mediated ubiquitination of IKKγ (also called NEMO)[18]. An alternative, TRAF6-independent mechanism of IKK activation has been proposed for the fusion protein of the caspase inhibitor c-IAP2 and MALT1, derived from t(11;18)-positive MALT lymphoma[20]. In that last study, the IKK-activating ability of the fusion protein was attributed to a direct NEMO-ubiquitination activity of MALT1 that depended on an immunoglobulin-like domain after the caspase-like domain[20]. Finally, two studies have noted that activation

[1]Department of Biochemistry, University of Lausanne, CH-1066 Epalinges, Switzerland. [2]Multidisciplinary Oncology Center, Lausanne University Hospital, CH-1005 Lausanne, Switzerland. [3]Present address: University Medical Center, CH-1211 Geneva 4, Switzerland. [4]These authors contributed equally to this work. Correspondence should be addressed to M.Th. (margot.thomemiazza@unil.ch).

Received 21 December 2007; accepted 22 January 2008; published online 10 February 2008; doi:10.1038/ni1568

of NF-κB by coexpression of MALT1 and Bcl-10 or expression of c-DAP2–MALT1 fusion proteins in nonlymphoid cells is substantially impaired by substitution of the predicted active-site cysteine residue of the caspase-like domain of MALT1 (refs. 21,22). Although that last finding indicates an important function for the putative active-site cysteine residue of MALT1, earlier attempts to demonstrate caspase-like proteolytic activity led to the conclusion that MALT1 does not have aspartate-specific proteolytic activity[23]. However, those studies did not formally exclude the existence of a proteolytic activity of MALT1 with distinct substrate specificity. It is notable in this context that members of the structurally related metacaspase family, in particular those found in plants and *Leishmania major*, have been shown to have arginine- or lysine-specific proteolytic activity[24–26].

Here we investigate the molecular function of MALT1 and Bcl-10 and identify MALT1 as an arginine-specific, cysteine-dependent protease that cleaves its substrate Bcl-10 after engagement of the T cell antigen receptor (TCR). The proteolytic activity of MALT1 was required for optimal NF-κB activation and production of interleukin 2 (IL-2), whereas MALT1-dependent cleavage of Bcl-10 specifically controlled integrin-dependent T cell adhesion. Thus, we have identified new functions and physiological roles for MALT1 and its substrate Bcl-10 that contribute to lymphocyte activation and thus, potentially, to lymphomagenesis.

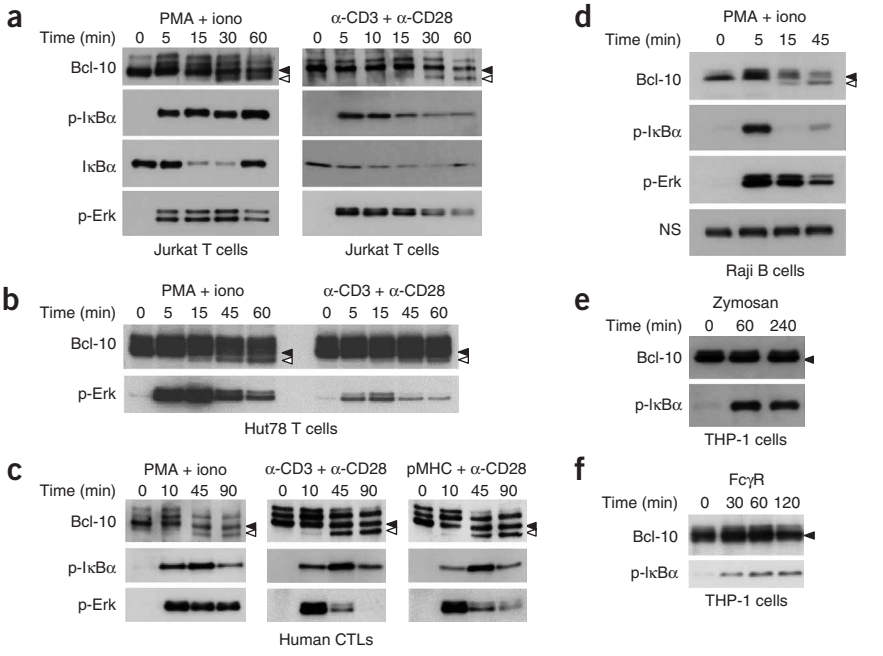

Figure 1 Lymphocyte activation induces Bcl-10 cleavage. (**a**–**d**) Immunoblot analysis of lysates of Jurkat T cells (**a**), Hut78 T cells (**b**), human cytomegalovirus-specific CD8$^+$ T lymphocytes (CTLs; **c**) or Raji B cells (**d**) left untreated (0) or stimulated with PMA and ionomycin (PMA + iono; **a**–**d**) or crosslinked anti-CD3 and anti-CD28 (α-CD3 + α-CD28; **a**–**c**) or multimers of polypeptide 65 and HLA-A*0201 plus anti-CD28 (pMHC + α-CD28; **c**) for various times (above lanes). (**e**,**f**) Immunoblot analysis of lysates of THP-1 cells left untreated (0) or treated with zymosan (**e**) or with crosslinked antibody to the Fc receptor (FcγR; **f**) for various times (above lanes). Filled arrowheads indicate the position of unmodified Bcl-10; open arrowheads indicate a faster migrating form of Bcl-10. p-, phosphorylated. Data are representative of three (**a**,**b**,**d**–**f**) or two (**c**) experiments.

RESULTS

Lymphocyte activation induces a smaller Bcl-10 isoform

To identify previously unknown post-translational modifications of Bcl-10 and to thereby gain further insight into its molecular function, we analyzed extracts of Jurkat and Hut78 human T cell lines that we stimulated with phorbol 12-myristate 13-acetate (PMA) and ionomycin or with antibody to CD3 (anti-CD3) and anti-CD28. Analysis of the extracts by high-resolution SDS-PAGE[27] identified a faster migrating Bcl-10 isoform that began to appear after 15 min of stimulation (**Fig. 1a**,**b**). The appearance of this Bcl-10 isoform was delayed relative to IκB phosphorylation (**Fig. 1a**), and it persisted for several hours after TCR engagement (**Supplementary Fig. 1** online) and did not require new protein synthesis (**Supplementary Fig. 2** online). We also found generation of the faster migrating Bcl-10 isoform in antigen-specific CD8$^+$ human cytotoxic T lymphocytes (CTLs) stimulated with PMA and ionomycin, with anti-CD3 and anti-CD28, or specifically with multimers of peptide and major histocompatibility complex (**Fig. 1c**). Stimulation of human Raji B cells with PMA and ionomycin led to similar results (**Fig. 1d**), but we did not detect the generation of a faster migrating Bcl-10 isoform when we stimulated human THP-1 monocytes with the dectin-1 ligand zymosan or agonists of Fcγ receptors, which depend on Bcl-10 for NF-κB activation or actin polymerization, respectively[28,29] (**Fig. 1e**,**f**).

The shorter Bcl-10 fragment requires CARMA1 and MALT1

A key step in TCR-induced NF-κB activation is the association of Bcl-10 with its 'upstream' binding partner CARMA1 through a CARD-mediated interaction[9]. The accessibility of the CARD of CARMA1 is regulated by PKC-θ-mediated phosphorylation of CARMA1 (ref. 1). To assess the relevance of these events for the generation of the faster migrating Bcl-10 fragment, we preincubated Jurkat cells with the 'pan-PKC' inhibitor bisindolyl-maleimide VIII (BIM) or with Gö6976, an inhibitor of the classical (calcium-dependent) PKC-α, PKC-β and PKC-γ isoforms. Consistent with the described function for PKC-θ (a calcium-independent, 'new' PKC isoform) 'upstream' of the CARMA1–Bcl-10–MALT1 complex in T cells[1], BIM but not Gö6976 prevented the generation of the faster migrating Bcl-10 isoform (**Fig. 2a**). Moreover, its generation was prevented by silencing of CARMA1 mediated by short hairpin RNA (shRNA; **Fig. 2b**) and was decreased considerably by the expression of a dominant negative mutant of CARMA1 that is unable to bind Bcl-10 (ref. 9; **Fig. 2c**). Expression of a CARMA1 coiled-coil construct, which prevents the formation of CARMA1 oligomers[30], also had an inhibitory effect on the activation-induced decrease in the apparent molecular size of Bcl-10 (**Supplementary Fig. 3** online). These findings collectively suggest that formation of the faster migrating Bcl-10 isoform depends on its recruitment by CARMA1 and on the formation of CARMA1 oligomers.

Studies have identified Bcl-10 as a direct substrate of IKKβ and have supported the idea that IKK-mediated phosphorylation of Bcl-10 can act as a negative feedback loop in T cell activation by affecting the stability and function of the CARMA1–Bcl-10–MALT1 complex[15,31].

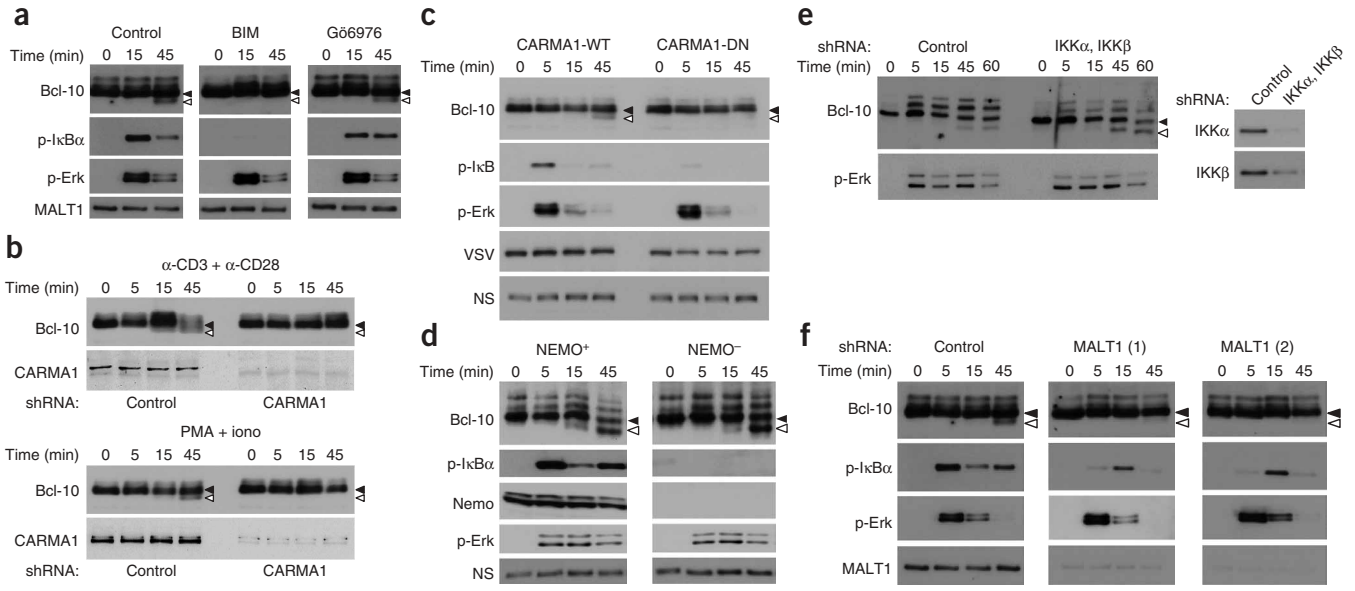

Figure 2 Molecular requirements for Bcl-10 cleavage. (**a**) Immunoblot analysis of lysates of Jurkat cells pretreated with the PKC inhibitors BIM or Gö6976 or with solvent control, followed by stimulation for 0, 15 or 45 min with anti-CD3 and anti-CD28. (**b**,**c**) Immunoblot analysis of lysates of Jurkat cells transduced with control (lamin A/C–specific) shRNA or CARMA1-specific shRNA (**b**) or with VSV-tagged wild-type CARMA1 (CARMA1-WT) or the dominant negative CARMA1 mutant (CARMA1-DN; **c**), then stimulated with anti-CD3 and anti-CD28 (**b**) or with PMA and ionomycin (**b**,**c**). (**d**–**f**) Immunoblot analysis of lysates of wild-type (NEMO$^+$) and NEMO-deficient (NEMO$^-$) Jurkat cells (**d**), or Jurkat cells stably transduced with lentiviral control (lamin A/C–specific) shRNA or IKKα- and IKKβ-specific shRNA (**e**) or two different MALT1-specific shRNA constructs (MALT1 (1) and (2); **f**), then stimulated with PMA and ionomycin (**d**,**e**) or anti-CD3 and anti-CD28 (**f**). (**e**) Right, evaluation of the efficiency of RNA silencing by immunoblot with anti-IKKα and anti-IKKβ. Filled and open arrowheads indicate the migration of uncleaved and cleaved Bcl-10, respectively; NS, nonspecific band (loading control). Slight differences in the resolution of bands in different panels result from sample analysis by either 15% SDS-PAGE by a published protocol[27] (**a**,**d**,**e**) or classical 11% SDS-PAGE (**b**,**c**,**f**). Data are representative of two (**a**,**c**,**d**) and three (**b**,**e**,**f**) experiments.

We analyzed NEMO-deficient Jurkat cells, as well as Jurkat cells in which expression of IKKα and IKKβ had been silenced, and found that after stimulation with PMA and ionomycin, the faster migrating Bcl-10 isoform was still detectable in cells lacking or having impaired expression of these proteins (**Fig. 2d**,**e**). Thus, signaling compounds acting 'upstream' of Bcl-10 are required, whereas NEMO and most likely IKKα and IKKβ are dispensable for generation of the observed Bcl-10 modification.

The Bcl-10-binding protein MALT1 has a caspase-like domain that shares homology with metacaspases[22], which have been identified as cysteine-dependent, arginine-specific proteases in plants[24,25] and *L. major*[26]. Therefore, we considered the possibility that MALT1 might be endowed with proteolytic activity and, because of its interaction with Bcl-10, could directly cleave Bcl-10 to generate a fragment with a smaller apparent molecular size. Indeed, silencing of MALT1 expression by two different shRNA molecules impaired the generation of the observed Bcl-10 modification (**Fig. 2f**), which suggested that the faster migrating Bcl-10 isoform might result from a MALT1-mediated proteolytic cleavage. Inhibition of proteasomal or caspase-type proteolytic activities did not affect Bcl-10 cleavage (**Supplementary Figs. 4** and **5** online). Therefore, it is unlikely that Bcl-10 cleavage was mediated by an indirect effect of MALT1 on these proteases.

MALT1-dependent cleavage of Bcl-10 after Arg228

To gain additional insight into the nature of the potential cleavage site of Bcl-10, we initially used two-dimensional gel electrophoresis to analyze lysates of unstimulated Jurkat T cells and Jurkat T cells stimulated with PMA and ionomycin (**Fig. 3a**). In both unstimulated and stimulated T cells, we noted the presence of unphosphorylated Bcl-10 together with two previously identified phosphorylation isoforms whose relative intensity increased after T cell activation, as described[29]. The cleaved form of Bcl-10 was present only in stimulated cell lysates; it migrated at an isoelectric point that was more acidic than that of the full-length form of Bcl-10 (**Fig. 3a**). This suggested that proteolytic cleavage occurred close to the carboxyl terminus of Bcl-10, which contains a positively charged arginine residue (Arg232) whose proteolytic removal could explain the more acidic isoelectric point (**Fig. 3b**). Therefore, we considered the possibility of MALT1-dependent cleavage after Arg228, which is conserved in both human and mouse Bcl-10 and is preceded by a serine residue that is also present in several metacaspase target cleavage sites (**Fig. 3b**). To test our hypothesis, we stably expressed wild-type Bcl-10 or a Bcl-10 mutant with substitution of glycine for the arginine at position 228 (R228G) in Jurkat cells and assessed the effect of stimulation with PMA and ionomycin on these constructs. Stimulation induced the formation of a faster migrating isoform for the Flag-tagged wild-type form but not the R228G mutant, which supported the idea of protease-dependent cleavage of Bcl-10 after Arg228 (**Fig. 3c**). We also noted processing of Bcl-10 when we expressed wild-type Bcl-10 together with MALT1 in 293T cells, but not with expression of the R228G mutant together with MALT1 (**Fig. 3d**), whereas point substitution of the neighboring residues Thr229, Val230 and Ser231 did not affect cleavage (**Supplementary Fig. 6** online). In this setting, Bcl-10 cleavage was dependent on the presence of the intact MALT1 caspase-like domain, as deletion of this domain or substitution of the putative active-site Cys464 of MALT1 (MALT1-C464A) abolished Bcl-10 cleavage (**Fig. 3d**). A MALT1 mutant in which the catalytically

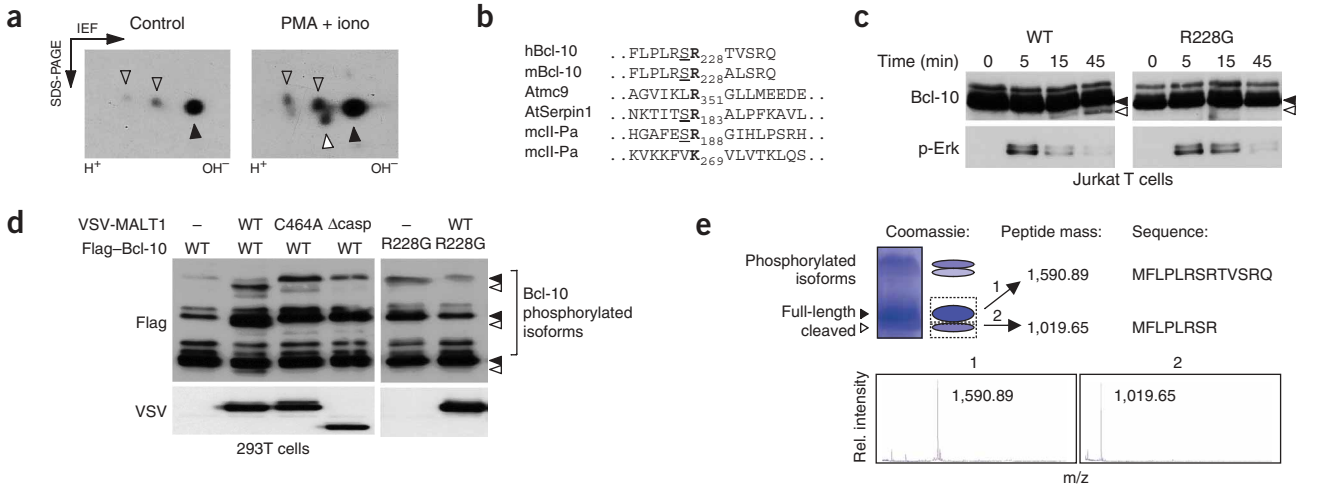

Figure 3 MALT1-dependent Bcl-10 cleavage occurs after Arg228. (**a**) Immunoassay of lysates of Jurkat T cells left unstimulated (Control) or stimulated for 30 min with PMA and ionomycin, analyzed by immunoblot with anti-Bcl-10 after two-dimensional gel electrophoresis. Filled arrowheads indicate unmodified Bcl-10; open arrowheads indicate previously described phosphorylation isoforms of Bcl-10 (ref. 29); white arrowhead (bottom right) indicates cleaved Bcl-10. IEF, isoelectric focusing. (**b**) Alignment of the carboxyl termini of human Bcl-10 (hBcl-10) and mouse Bcl-10 (mBcl-10) with the previously identified autoprocessing sites of the metacaspase of *A. thaliana* (Atmc9)[24], the cleavage site of the Atmc9 substrate Serpin1 (AtSerpin1)[32] and metacaspase type II of *P. abies* (mcII-Pa)[25]. (**c**) Immunoblot analysis of anti-Flag immunoprecipitates of Jurkat T cells transduced with lentiviral expression constructs of Flag-tagged wild-type Bcl-10 (WT) or the R228G mutant of Bcl-10, then left untreated (0) or stimulated with PMA and ionomycin. (**d**) Immunoblot analysis of lysates of 293T cells transfected with various Bcl-10 and MALT1 constructs (above lanes). Δcasp, deletion of the MALT1 caspase-like domain. (**e**) SDS-PAGE and Coomassie staining of immunoprecipitated Flag-tagged Bcl-10 from 293T cells cotransfected with VSV-MALT1 (top left); filled and open arrowheads indicate the positions of unmodified and cleaved Bcl-10, respectively. Bands corresponding to uncleaved and cleaved Bcl-10 were excised and analyzed by mass spectrometry (right and below). Uncleaved Bcl-10 contains the full-length carboxy-terminal Glu-C peptide of 1,590.89 Daltons (amino acids 220–233); the cleaved form of Bcl-10 contains a carboxy-terminal Glu-C peptide of 1,019.65 Daltons (amino acids 220–228). Data are representative of three experiments (**a**,**c**,**d**) or one experiment (**e**).

important residue His415 was substituted with alanine produced results similar to those of the MALT1-C464A mutant (data not shown). Finally, we confirmed Arg228 as the cleavage site by mass spectrometry of the carboxy-terminal peptide composition of the Bcl-10 cleavage isoforms immunoprecipitated from 293T cells transfected with Bcl-10 and MALT1 (**Fig. 3e**). These experiments collectively suggest that MALT1 acts as an arginine-specific protease that cleaves Bcl-10 after Arg228.

MALT1 is a cysteine-dependent protease

So far, our data demonstrated that a MALT1-dependent proteolytic activity was responsible for the observed cleavage of Bcl-10 after Arg228. To formally demonstrate proteolytic activity of purified MALT1 *in vitro*, we next set up an *in vitro* cleavage assay with purified recombinant glutathione *S*-transferase (GST), GST-MALT1 and GST–MALT1-C464A constructs immobilized on glutathione-Sepharose. Incubation of these beads with the Bcl-10-derived fluorogenic substrate 'LRSR-AMC' (a peptide substrate (Leu-Arg-Ser-Arg) mimicking the Bcl-10 cleavage site, conjugated to the fluorogen 7-amino-4-methylcoumarin (AMC)) resulted in peptide cleavage by the GST-MALT1 construct, which was abolished by substitution of the predicted active-site Cys464 with alanine (MALT1-C464A; **Fig. 4a**). In similar conditions, immobilized purified GST-MALT1, but neither GST–MALT1-C464A nor the GST control, induced cleavage of purified recombinant Bcl-10 *in vitro* (**Fig. 4b**).

Next we assessed the effect of T cell activation on the proteolytic activity of MALT1 with LRSR-AMC. Stimulation of Jurkat cells with PMA and ionomycin led to a specific increase in proteolytic activity that was impaired when MALT1 expression was silenced (**Fig. 4c**,**d**). The activation-induced increase in LRSR-AMC–cleavage activity correlated with an increase in the detection of cleaved endogenous Bcl-10 in the lysate; the cleaved form of Bcl-10 subsequently persisted, whereas the proteolytic activity decreased (**Fig. 4c**). The most likely interpretation of these findings is that T cell activation leads to a transient activation of the proteolytic activity of MALT1 that allows the formation of a long-lived cleaved form of Bcl-10 (**Supplementary Fig. 1**). In similar conditions, no inducible cleavage of the caspase-3 substrate DEVD-AMC (Asp-Glu-Val-Asp conjugated to AMC) was detectable (**Fig. 4c**). Finally, we designed an inhibitor, z-VRPR-fmk, based on the published optimal tetrapeptide substrate Val-Arg-Pro-Arg of the *Arabidopsis thaliana* metacaspase AtmC9 (ref. 32) conjugated to fluoromethyl ketone (fmk), and tested its effect on the *in vitro* activity of recombinant MALT1 and on the T cell activation–induced cleavage of Bcl-10. We found that z-VRPR-fmk inhibited the LRSR-AMC–cleavage activity of GST-MALT1 in a dose-dependent way (**Fig. 4e**). Moreover, preincubation of Jurkat cells and human antigen-specific CTLs with the inhibitor prevented the activation-induced cleavage of Bcl-10 (**Fig. 4f**,**g**). These findings collectively suggest that MALT1 acts as a cysteine-dependent, arginine-specific protease whose activity increases transiently after T cell activation to allow the formation of a carboxy-terminally cleaved form of Bcl-10.

Proteolytic MALT1 is required for optimal NF-κB activation

To assess the effect of MALT1 inhibition on T cell activation, we did NF-κB reporter assays of Jurkat cells that we treated with z-VRPR-fmk 30 min before and during stimulation (**Fig. 5a–c**). Treatment of the cells with 75 μM z-VRPR-fmk inhibited activation of a classical NF-κB reporter construct, with anti-CD3 and anti-CD28 or with PMA and ionomycin as activating stimuli (**Fig. 5a**,**b**). We obtained similar results with Jurkat cells activated with Raji B cells, which can present

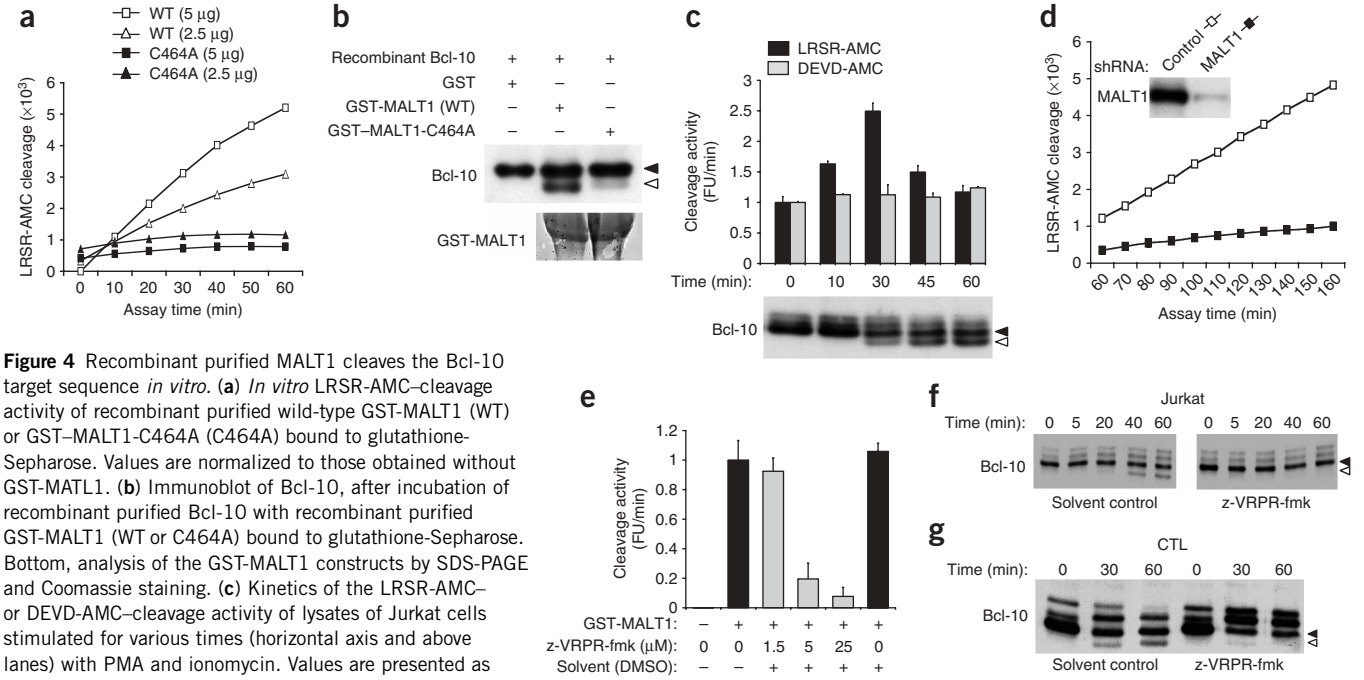

Figure 4 Recombinant purified MALT1 cleaves the Bcl-10 target sequence *in vitro*. (**a**) *In vitro* LRSR-AMC–cleavage activity of recombinant purified wild-type GST-MALT1 (WT) or GST–MALT1-C464A (C464A) bound to glutathione-Sepharose. Values are normalized to those obtained without GST-MATL1. (**b**) Immunoblot of Bcl-10, after incubation of recombinant purified Bcl-10 with recombinant purified GST-MALT1 (WT or C464A) bound to glutathione-Sepharose. Bottom, analysis of the GST-MALT1 constructs by SDS-PAGE and Coomassie staining. (**c**) Kinetics of the LRSR-AMC– or DEVD-AMC–cleavage activity of lysates of Jurkat cells stimulated for various times (horizontal axis and above lanes) with PMA and ionomycin. Values are presented as fluorescence units (FU) per unit time (mean + s.d. of triplicate determinations) and are normalized to the protein content of lysates. Below, immunoblot analysis of Bcl-10 cleavage. (**d**) LRSR-AMC–cleavage activity of lysates of Jurkat cells transduced with lentivirus with control (lamin A/C–specific) shRNA or MALT1-specific shRNA, then incubated for 20 min with or without PMA and ionomycin; values are normalized to those of unstimulated controls. Values are normalized to those obtained with lysis buffer only. Inset, immunoblot analysis of the efficiency of MALT1 silencing. (**e**) *In vitro* LRSR-AMC–cleavage activity of recombinant purified GST-MALT1 bound to glutathione-Sepharose, in the presence or absence of 0–25 μM z-VRPR-fmk. (**f**,**g**) Immunoblot analysis of lysates of Jurkat cells (**f**) or human antigen-specific CTLs (**g**), preincubated with 75 μM z-VRPR-fmk or DMSO (Solvent control), then stimulated for 0–60 min with PMA and ionomycin in the continued presence or absence of the inhibitor. Filled and open arrowheads indicate unmodified and cleaved Bcl-10, respectively. Data are representative of three (**a**,**c**,**f**) or two (**b**,**d**,**e**,**g**) experiments.

the staphylococcus enterotoxin E (SEE) 'superantigen' to the $V_\beta8^+$ Jurkat T cell clone J77.20 we used in this study (**Fig. 5c**). Moreover, inactivation of MALT1 catalytic activity by deletion of the caspase-like domain or substitution of the active-site residues Cys464 or His415 led to partially impaired activation of an NF-κB reporter construct in 293T cells (**Supplementary Fig. 7** online), consistent with published reports describing impaired NF-κB activation by the corresponding cysteine mutant of MALT1 (refs. 21,22). Thus, the proteolytic activity of MALT1 is required for optimal NF-κB activation.

MALT1 and Bcl-10 have been shown to promote activation of the NF-κB c-Rel subunit in B cells[33]. In T cells, c-Rel contributes to optimal activation and cytokine production by binding to the CD28 response element that is present in the promoter of *Il2* and of additional genes controlling T cell activation[34]. Using a CD28 response element reporter construct, we also noted partial but substantial inhibition of activation of this element after treatment with z-VRPR-fmk and stimulation with either PMA and ionomycin or SEE-presenting Raji cells (**Fig. 5d**,**e**). Finally, we assessed the effect of the inhibitor on activation-induced IL-2 secretion by both Jurkat cells and human antigen-specific CTLs. Treatment of Jurkat cells with z-VRPR-fmk led to considerable dose-dependent inhibition of IL-2 secretion induced by SEE-presenting Raji cells (**Fig. 5f**). Moreover, we noted partial inhibition of IL-2 secretion by human CTLs from two different donors after stimulation with PMA and ionomycin (**Fig. 5g**). Notably, the inhibitor did not affect the stimulation-induced phosphorylation of IκBα or the kinases Jnk and Erk, which occurs before optimal MALT1 activation (**Supplementary Fig. 8** online). Moreover, the inhibitor did not modulate the upregulation of CD69 induced by PMA and ionomycin in Jurkat cells (data not shown). Finally, it is important to note that prolonged treatment of the cells with up to 200 μM z-VRPR-fmk did not affect the viability of the cells and they showed no sign of morphological alteration (data not shown). These findings collectively suggest that inhibition of the proteolytic activity of MALT1 by z-VRPR-fmk impairs the TCR-induced activation of NF-κB and production of IL-2.

Bcl-10 cleavage is crucial for adhesion to fibronectin

To assess whether MALT1-dependent Bcl-10 cleavage was responsible for the effects on gene transcription described above, we next tested whether expression of the noncleavable Bcl-10 isoform (the R228G mutant) affected TCR-induced NF-κB responses. First we compared the capacity of wild-type Bcl-10 and the R228G mutant to reconstitute the activation of a classical NF-κB reporter construct in Jurkat cells with silenced expression of endogenous Bcl-10. After stimulation of the cells with PMA and ionomycin or with SEE-presenting Raji B cells, the R228G mutant was fully able to restore NF-κB activation in the 'Bcl-10-silenced' cells (**Fig. 6a**,**b**). Moreover, we found that the R228G mutant was similar to wild-type Bcl-10 in its capacity to promote transcription dependent on the CD28 response element (**Fig. 6c**) and transcription of an *Il2* reporter gene (data not shown). These findings collectively suggest that activation of the NF-κB pathway by antigen-presenting cells or by drugs that mimic the antigen receptor signal does not require MALT1-dependent cleavage of Bcl-10 but most likely depends on other MALT1 substrates.

Because Bcl-10 cleavage depended on PKC activity (**Fig. 2a**), we next considered involvement of cleaved Bcl-10 in other PKC-dependent

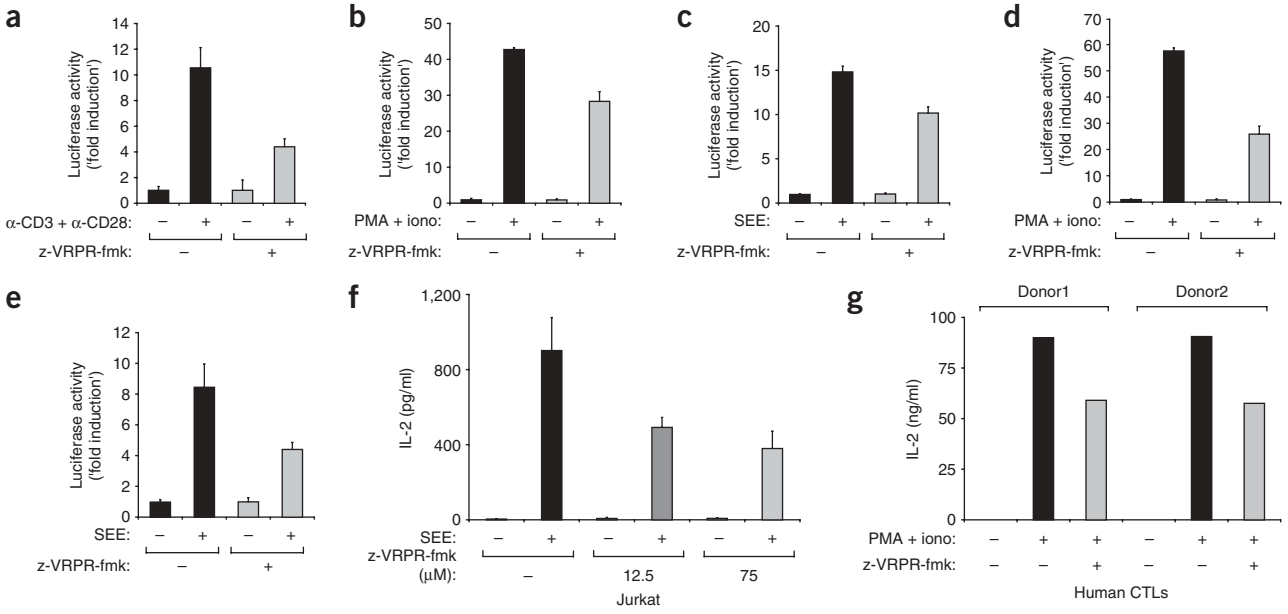

Figure 5 Inhibition of the proteolytic activity of MALT1 impairs activation-induced NF-κB and IL-2 responses. (**a**–**e**) Reporter assays of Jurkat cells transfected with firefly luciferase constructs of NF-κB (**a**–**c**) or the CD28 response element (**d**,**e**) plus a renilla luciferase construct, then, 24 h later, resuspended for 30 min in fresh medium containing 75 μM z-VRPR-fmk or equivalent solvent (DMSO) control before stimulation for 16 h, in the continued presence or absence of the inhibitor, with cross-linked anti-CD3 and anti-CD28 (**a**), PMA and ionomycin (**b**,**d**) or SEE-presenting Raji cells (**c**,**e**). Luciferase activity is presented relative to basal activity. (**f**,**g**) IL-2 concentrations in supernatants of Jurkat cells (**f**) or human antigen-specific $CD8^+$ T cells (**g**) preincubated for 30 min with solvent control (DMSO), 12.5 μM z-VRPR-fmk (**f**) or 75 μM z-VRPR-fmk (**f**,**g**), then stimulated for 16 h with SEE-loaded Raji cells (**f**) or PMA and ionomycin (**g**) in the continued presence or absence of the inhibitor. Data are representative of three experiments (**a**–**f**; mean + s.d.) or are the average of duplicate determinations for two different donors (**g**).

signaling events in T cell activation, such as the stimulation-induced, integrin-mediated adhesion of T cells[35]. The β_1 integrins $\alpha_4\beta_1$ (VLA-4) and $\alpha_5\beta_1$ (VLA-5) and the β_2 integrin $\alpha_L\beta_2$ (LFA-1) have well described functions in T cell adhesion and costimulation[36,37]. We focused our attention on β_1 integrins, as we did not see much effect of Bcl-10 cleavage on NF-κB activation in Jurkat cells after stimulation with SEE-presenting Raji cells (**Fig. 6b**), which is expected to be sensitive to conjugate formation and costimulation mediated by $\alpha_L\beta_2$ and its ligand ICAM-1 (ref. 38). In Jurkat T cells, adhesion to the β_1 ligand fibronectin is mediated mainly by the integrin $\alpha_4\beta_1$, with a minor contribution from $\alpha_5\beta_1$ (refs. 35,39). First we assessed the relevance of MALT1 and its substrate Bcl-10 to the adhesion of T cells to fibronectin. Silencing of the expression of MALT1 or Bcl-10 by RNA-mediated interference decreased the activation-induced adhesion of Jurkat cells to fibronectin (**Fig. 6d**). Manganese-induced adhesion, in contrast, was not affected much by the silencing of MALT1 or Bcl-10 (**Fig. 6d**). Next we compared the adhesion to fibronectin of Jurkat cells stably expressing either wild-type Bcl-10 or the noncleavable R228G mutant (**Supplementary Fig. 9** online) and an shRNA construct specific only for endogenous Bcl-10 (that is, neither stably expressed Bcl-10 mRNA was targeted by the silencing vector). After activation with either anti-CD3 and anti-CD28 or PMA, cells expressing the R228G mutant had less adhesion to fibronectin than did cells expressing wild-type Bcl-10 (**Fig. 6e**). In contrast, manganese-induced adhesion was similar in cells expressing wild-type Bcl-10 or the R228G mutant (**Fig. 6e**).

Finally, we assessed the effect of the MALT1 inhibitor z-VRPR-fmk on the adhesion of T cells to fibronectin. Pretreatment of Jurkat cells with z-VRPR-fmk decreased the capacity of the cells to adhere to fibronectin after stimulation with anti-CD3 and anti-CD28 or after PMA treatment, but it did not affect manganese-induced adhesion (**Fig. 6f**). Moreover, we noted partial but reproducible inhibition of adhesion of T cells to fibronectin induced by anti-CD3 and anti-CD28 in human CTLs from two different donors (**Fig. 6g**). The less potent effect of the inhibitor on primary cells versus Jurkat cells, also noted for IL-2 production (**Fig. 5f**,**g**), might have been due to lower permeability of the primary T cells to the inhibitor or to a shorter half-life of the inhibitor in the CTLs, which contain high proteolytic activity that may rapidly degrade the inhibitor peptide. The results reported above collectively support the idea that MALT1-dependent Bcl-10 cleavage is essential in the activation-induced adhesion of T cells to the β_1 integrin ligand fibronectin.

Integrin-mediated adhesion is generally thought to be regulated by activation-induced conformational changes that modulate integrin affinity and by affinity-independent mechanisms, such as lateral diffusion and clustering of integrins, alterations in cytoskeletal associations, and changes in integrin expression patterns[40]. However, the exact mechanism underlying $\alpha_4\beta_1$ (VLA-4) activation remains poorly understood. Analysis by flow cytometry showed that surface expression of β_1 integrin was similar in cells expressing wild-type or noncleavable (R228G) Bcl-10 (data not shown). Moreover, these Jurkat cell populations had indistinguishable, constitutive amounts of the high-affinity conformation of $\alpha_4\beta_1$ detectable by recombinant $\alpha_4\beta_1$ ligand VCAM-1 fused to the Fc region of an antibody. These amounts did not increase further after treatment with PMA and ionomycin (data not shown), consistent with published findings[41]. In addition, we noted indistinguishable, constitutive clustering of the β_1 integrin in unstimulated Jurkat cells or Jurkat cells treated with PMA and ionomycin in the presence or absence of z-VRPR-fmk (data not shown). Together with the observation that Bcl-10 cleavage

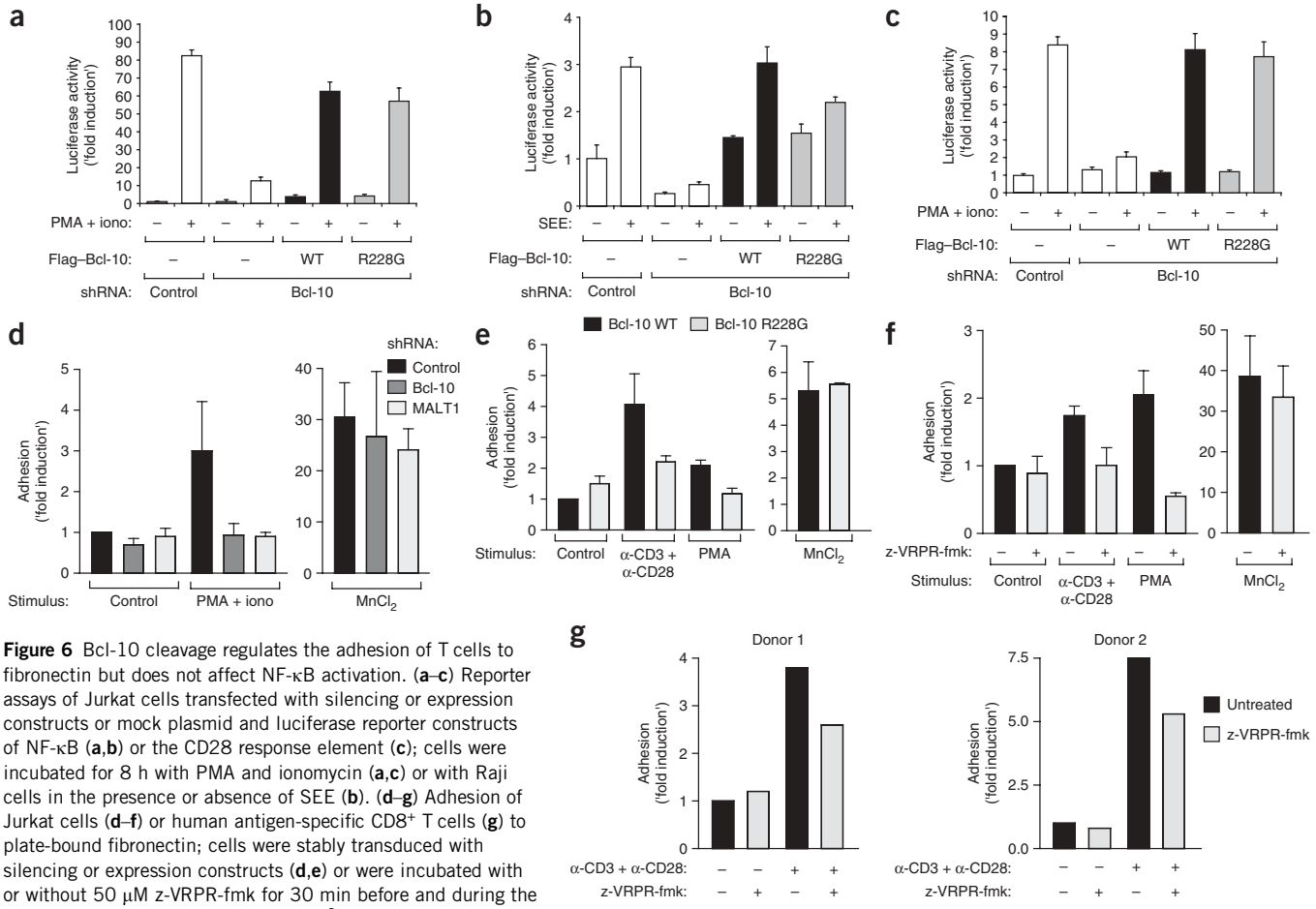

Figure 6 Bcl-10 cleavage regulates the adhesion of T cells to fibronectin but does not affect NF-κB activation. (**a**–**c**) Reporter assays of Jurkat cells transfected with silencing or expression constructs or mock plasmid and luciferase reporter constructs of NF-κB (**a**,**b**) or the CD28 response element (**c**); cells were incubated for 8 h with PMA and ionomycin (**a**,**c**) or with Raji cells in the presence or absence of SEE (**b**). (**d**–**g**) Adhesion of Jurkat cells (**d**–**f**) or human antigen-specific $CD8^+$ T cells (**g**) to plate-bound fibronectin; cells were stably transduced with silencing or expression constructs (**d**,**e**) or were incubated with or without 50 μM z-VRPR-fmk for 30 min before and during the assay (**f**,**g**), or were stimulated with Mn^{2+} (right) for 15 min (**d**,**f**) or 30 min (**e**). Data (mean + s.d.) are representative of three experiments (**a**–**c**), three experiments for control and Bcl-10-specific shRNA and two experiments for MALT1-specific shRNA (**d**), three experiments for anti-CD3 and anti-CD28, four experiments for PMA, and two experiments for Mn^{2+} (**e**), four or more experiments (**f**), or two different donors (**g**).

reached a maximum at approximately 30–60 min after T cell activation (**Fig. 1**), these findings suggest that cleavage of Bcl-10 might not modulate integrin affinity but instead may affect an event that happens after receptor occupancy, such as changes in cytoskeletal interactions that might affect the stability of the interaction of the integrin with its ligand.

DISCUSSION

Here we have provided several lines of evidence identifying MALT1 as an arginine-specific protease that directly cleaves its substrate Bcl-10 after T cell activation. First, MALT1 was required for activation-induced cleavage of Bcl-10 in T cells. Second, a recombinant active form of MALT1 cleaved recombinant purified Bcl-10 *in vitro*. Third, substitution of the predicted active site cysteine residue of MALT1 prevented Bcl-10 cleavage. Fourth, a cell-permeable peptide inhibitor that impaired MALT1 activity prevented Bcl-10 cleavage in both Jurkat T cells and primary human CTLs. Fifth, mass spectrometry and mutational characterization of the Bcl-10 cleavage site identified Arg228 as a conserved residue that directly precedes the site of cleavage. Finally, substitution of the cleavage-site arginine with glycine impaired MALT1-dependent cleavage of Bcl-10 and inhibited T cell activation–induced adhesion of the cells to the $\alpha_4\beta_1$ (VLA-4) ligand fibronectin. Our results identify a previously unknown proteolytic activity for MALT1 and identify MALT1-dependent Bcl-10 cleavage as a key event in TCR-induced, β_1 integrin–mediated adhesion.

The identification of MALT1 as an arginine-specific protease is consistent with the original description of MALT1 as a protein that shares sequence similarity with proteases of the caspase family as well as with other caspase-related proteins of the metacaspase family[22,42]. In fact, the cleavage of Bcl-10 after Arg228 by MALT1 is analogous to the previously described arginine-lysine–specific proteolytic activity of metacaspases of plants and *L. major*[24–26], which show the highest sequence similarity with MALT1 of the known cysteine-dependent protease families[22]. Our study also provides insight into the molecular mechanism underlying MALT1 activation. Inhibition of PKC-θ activity or silencing of CARMA1 led to impaired Bcl-10 cleavage, which suggests that PKC-θ-dependent CARMA1–Bcl-10–MALT1 complex assembly is required for MALT1 activation and Bcl-10 cleavage. Notably, inhibition of coiled-coil–mediated formation of CARMA1 oligomers also inhibited Bcl-10 cleavage. This suggests that the oligomeric CARMA1 scaffold is crucial for MALT1 activation, most likely through the induced-proximity mechanism proposed for caspase activation[43].

We designed the cell-permeable, irreversible inhibitor z-VRPR-fmk (an inhibitor analogous to the well known caspase inhibitor z-VAD-fmk) based on the sequence of a published optimal tetrapeptide substrate for the *A. thaliana* metacaspase AtMC9 (ref. 32). With this

inhibitor, we have also provided evidence of involvement of MALT1 proteolytic activity in TCR-induced NF-κB activation and IL-2 production. Although the MALT1 substrate responsible for this effect remains to be identified, our data indicate the presence of an important, as-yet-unexplored signaling mechanism that controls NF-κB activation independently of the initial TCR-induced IKK-mediated phosphorylation of IκB.

The biochemical identification of a proteolytic substrate of MALT1, its binding partner Bcl-10, allowed us to identify an additional, NF-κB-independent function for MALT1 in T cell activation. Treatment of cells with the MALT1 inhibitor z-VRPR-fmk or substitutional inhibition of Bcl-10 cleavage resulted in less adhesion of Jurkat cells to fibronectin induced by anti-CD3 and anti-CD28 or by PMA. In contrast, cleavage of Bcl-10 did not affect its capacity to support TCR-induced NF-κB activation. Thus, the proteolytic activity of MALT1 controls both transcription-dependent and transcription-independent mechanisms of T cell activation.

Adhesion of the two T cell β_1 integrins VLA-4 and VLA-5 to their natural ligands, the extracellular matrix protein fibronectin and the cellular counter-receptors VCAM-1 and junctional adhesion molecules, is believed to be crucial not only for the migration of T cells to inflamed tissues but also for the stabilization of T cell–antigen-presenting cell contact and for the transduction of costimulatory T cell signals[36,38]. Consistent with the last ideas is the observation that $\alpha_4\beta_1$ (VLA-4) concentrates at the peripheral supramolecular activation cluster of Raji-Jurkat conjugates[44], although it remains unknown whether a suitable VLA-4 counter-receptor is expressed on the antigen-presenting Raji cells used in that study[44]. On the basis of our data, it is possible that the status of Bcl-10 cleavage might affect integrin-dependent T cell priming and/or extravasation, and this might at least in part account for the reported observation that Bcl-10-deficient mice show impaired footpad swelling in response to lymphocytic choriomeningitis virus[45], a primary immune reaction that is attributed to the infiltration of $CD8^+$ cytotoxic T lymphocytes. Future work should further delineate the individual contributions of MALT1 and Bcl-10 to NF-κB-dependent and NF-κB-independent mechanisms of the adaptive immune response.

In conclusion, our work has identified a proteolytic activity of MALT1 that is key to NF-κB activation. We have also defined a selective function for the MALT1-dependent cleavage of its substrate Bcl-10 in TCR-induced integrin adhesion. Our findings indicate that the proteolytic activity of MALT1 is a potential target for the development of immunomodulatory drugs and agents that combat lymphoma progression.

METHODS

Antibodies. Primary antibodies used in this study included monoclonal mouse anti-Flag (M2), rabbit anti-Flag (F7425), monoclonal mouse antibody to vesicular stomatitis virus (anti-VSV; P5D4), mouse antibody to phosphorylated Erk (MAPK-YT), rabbit anti-IκBα (9242) and mouse anti-tubulin (B-5-1-2; all from Sigma); monoclonal antibody to phosphorylated IκBα (5A5; Cell Signaling); rabbit antibody to phosphorylated Jnk (44-682G; Biosource); rabbit anti–NEMO (FL-419), mouse anti-IKKα (B78-1), rabbit anti-Bcl-10 (H-197) and mouse anti-IKKβ (S-20; all from Santa Cruz Biotechnology); mouse anti–caspase-8 (5F7; MBL); rabbit anti-PARP (9542; Cell Signaling); rabbit anti-CARMA1 (AL220; Alexis); and affinity-purified anti-MALT1 generated against a GST-MALT1 fusion protein composed of amino acids 1–824 of human MALT1. Horseradish peroxidase–coupled goat anti-mouse or anti-rabbit were from Jackson Immunoresearch.

Plasmids. Bcl-10 point mutants and MALT1 mutants (C464A, substitution of His415 with alanine, and the mutant lacking the caspase-like domain (amino acids 348–561)) were generated by a standard double-PCR approach, then were subcloned into expression vectors derived from pCR3 (Invitrogen) and verified by sequencing in both directions before further subcloning into the lentiviral vector pRDI_292 (a gift from R. Iggo), which allows expression of constructs under control of the promoter of *Eef1a1* (elongation factor 1). The luciferase–CD28 response element 'pCD28RE-LUC' reporter was constructed by cloning of an oligonucleotide containing four copies of the composite CD28RE-NF-IL-2B AP-1-binding site (5′-TTTAAAGAAATTCCAAAGAGTCATCA-3′; ref. 46) into the pGL3-Promoter vector (Promega).

Cells. The human cell lines Jurkat (J77 clone 20), Hut78 and Raji (gifts from O. Acuto) and THP-1 cells (American Type Culture Collection) were grown at 37 °C in RPMI 1640 medium supplemented with 10% (vol/vol) FCS and antibiotics. Jurkat cells expressing VSV-tagged wild-type CARMA1 or the dominant negative mutant of CARMA1 (L39R substitution of CARD) have been described[9]. Jurkat cells expressing a VSV-tagged construct encompassing the CARMA1 coiled-coil region (amino acids 106–445) were generated by retroviral transduction and puromycin selection[9]. Blood samples obtained from two healthy HLA-A*0201$^+$ volunteers contained readily detectable frequencies of $CD8^+$ T cells specific for Epstein-Barr virus and cytomegalovirus by *ex vivo* analyses. Peripheral blood mononuclear cells were obtained by density centrifugation with Ficoll-Hypaque (Pharmacia) and were cryopreserved in RPMI 1640 medium supplemented with 40% (vol/vol) FCS and 10% (vol/vol) DMSO (1×10^7 to 2×10^7 cells per vial) until further use. All healthy donors in this study provided informed consent. Phycoerythrin-labeled HLA-A*0201 peptide multimers were prepared with NLVPMVATV peptide (cytomegalovirus polypeptide 65, amino acids 495–503) and were provided by P. Guillaume and I. Luescher. Multimer-positive $CD8^+$ T cells were sorted with a FACSVantage and CellQuest software (Becton Dickinson) and their populations were expanded in RPMI 1640 medium supplemented with 8% (vol/vol) human serum, recombinant human IL-2 (150 U/ml; a gift from GlaxoSmithKline), phytohemagglutinin (1 μg/ml; Sodiag) and irradiated (3,000 rads) allogeneic peripheral blood mononuclear cells as feeder cells (1×10^6 cells/ml). Multimer-positive cytomegalovirus-specific T cells in 24-well plates were periodically restimulated (every 15 d) with phytohemagglutinin, irradiated feeder cells and recombinant human IL-2.

Transfection and transduction of cells. Transient transfection of 293T cells and lentiviral transduction of Jurkat T cells were done as described[29]. Transient transfection of Jurkat cells was accomplished by electroporation (260 V and 950 μF) in PBS supplemented with $CaCl_2$ and $MgCl_2$ (Gibco); this yielded transfection efficiencies of approximately 10–20%.

Silencing of protein expression. Lentiviral silencing vectors specific for CARMA1, Bcl-10 and MALT1 have been described[29]. A second, independent MALT1-silencing vector was from OpenBiosystems (TRCN0000073826). Silencing vectors targeting the α- and β-subunits of IKK were provided by Y. Refaeli, and Jurkat cells deficient in IKKγ (NEMO) and the parental control cells were provided by A. Ting.

Cell activation and lysis. T cell stimulation was initiated by the addition of PMA (10 ng/ml; Alexis) and ionomycin (1 μM; Calbiochem) or a combination of anti–human CD3ε (10 μg/ml of OKT3; Apotech) and anti-CD28 (10 μg/ml of CD28.2; Immunotech), followed immediately by the addition of crosslinking goat anti-mouse (5 μg/ml; Jackson Laboratories). In some experiments, Jurkat cells were stimulated by being mixed with Raji cells (at a cell/cell ratio of 1:1) in the presence or absence of recombinant SEE (100 ng/ml; Toxin Technology). For short-term stimulation (up to 1 h), cells were resuspended at a density of 2×10^7 cells per ml in RPMI medium with 0.5% (vol/vol) serum and were prewarmed for 10 min at 37 °C before the addition of the stimulating reagent. Longer stimulations were done at a density of 1×10^6 cells per ml in RPMI medium with 10% (vol/vol) serum. In some experiments, cells were preincubated for 30 min at 37 °C with 25 μM z-VAD-fmk or various concentrations of z-VRPR-fmk (Alexis Biochemicals), PKC inhibitors (5 μM Gö6976 (Calbiochem) or 500 nM bisindoleylmaleimide VIII acetate (Alexis)), 5 μM MG132 (Calbiochem), 10 μg/ml of cycloheximide (Sigma) or with corresponding volume of solvent, directly before stimulation. Human cytomegalovirus-specific

T lymphocytes were stimulated with multimers of peptide and major histocompatibility complex (10 μg/ml; polypeptide 65, amino acids 495–503, of HLA-A*0201) together with anti-CD28 (10 μg/ml; CD28.2; Immunotech). Raji B cells were stimulated with PMA (10 ng/ml; Alexis) and ionomycin (1 μM; Calbiochem). THP-1 cells were stimulated with zymosan (200 μg/ml; Sigma) or anti-FcγR Fab (20 μg/ml; IV.3 hybridoma; American Type Culture Collection), followed immediately by crosslinking with goat anti-mouse $F(ab')_2$ (10 μg/ml; Jackson ImmunoResearch). Stimulation was stopped by the addition of ice-cold Tris-NaCl buffer (20 mM Tris-HCl, pH 7.4, and 150 mM NaCl), and pelleted cells were lysed in Tris-NaCl lysis buffer containing 1% (vol/vol) Nonidet P-40, protease inhibitors (Complete; Roche) and phosphatase inhibitors (Cocktails I and II; Sigma). Transfected 293T cells were washed in cold Tris-NaCl buffer and were lysed in Tris-NaCl lysis buffer. Postnuclear cell lysates were boiled with reducing SDS sample buffer and were analyzed by SDS-PAGE. For optimal resolution of Bcl-10 isoforms, samples were analyzed on 16-cm × 20-cm gels by 15% SDS-PAGE according to a published protocol[27], except where indicated otherwise.

Two-dimensional electrophoresis, reporter assays and enzyme-linked immunosorbent assay. Two-dimensional protein analysis, NF-κB luciferase assays and measurement of IL-2 concentrations by enzyme-linked immunosorbent assay were done as described[29].

Identification of the Bcl-10 cleavage site. Pooled lysates from ten 10-cm dishes of 293T cells transfected with Flag-tagged Bcl-10 or with Flag-tagged Bcl-10 plus VSV-tagged MALT1 were used for anti-Flag immunoprecipitation on anti-Flag–agarose (Sigma). Samples were processed by 15% SDS-PAGE as published[27], and Coomassie-stained bands corresponding to uncleaved and cleaved Bcl-10 were cut out and analyzed by in-gel endoproteinase digestion with the endoproteinase. Glu-C and mass spectrometry (MALDI-MS; TOPLAB).

***In vitro* protease activity assay.** Unstimulated Jurkat T cells or Jurkat T cells stimulated with PMA and ionomycin were mechanically lysed in cleavage assay buffer (50 mM Tris-HCl, pH 7.4, 60 mM NaCl, 10 mM KCl, 20 mM $MgCl_2$, 100 mM $CaCl_2$ and 10 mM dithiothreitol) with a Dounce homogenizer. MALT1 protease activity was determined with a Synergy microplate reader (BioTek) after the addition of 50 μM amino-terminally acetylated (Ac-) peptide substrate Ac-LRSR-AMC (Peptides International) and incubation for 4 h at 30 °C. Caspase activity was assessed in the same conditions with 25 μM Ac-DEVD-AMC (Biomol International). Similar experiments were done to detect the proteolytic activity of recombinant purified GST-MALT1 (wild-type or C464A) bound to glutathione-Sepharose (Sigma). For the generation of GST-MALT1, full-length human MALT1 cDNA (wild-type or C464A) was cloned in-frame into pGEX-6P-1 (GE Healthcare). Plasmids were transformed in *Escherichia coli* BL21 bacteria and expression of GST fusion proteins was induced for 16 h at 18 °C in logarithmically growing bacteria with 0.04 mM isopropyl β-D-thiogalactopyranoside. Bacteria were collected and lysed, with a French press, in lysis buffer containing 50 mM HEPES, pH 7.9, 300 mM NaCl, 1 mM EDTA, 0.1% (vol/vol) Nonidet P-40, 1 mM dithiothreitol and aprotinin (2 μg/ml; Applichem). GST-MALT1 proteins were immobilized for 16 h at 4 °C on glutathione-Sepharose beads (GE Healthcare). Beads were washed extensively, were stored in lysis buffer at 4 °C and were used within 24 h of preparation. Aliquots of beads were assessed for GST-MALT1 protein content by being boiled in SDS sample buffer, separated by SDS-PAGE and stained with Coomassie blue. For analysis of the *in vitro* proteolytic activity of MALT1 on purified protein substrate, 75 ng recombinant Bcl-10 (Jena Bioscience) was incubated for 4 h at 20 °C with 5 μg recombinant purified GST-MALT1 (wild-type or C464A) immobilized on glutathione-Sepharose in cleavage assay buffer, and cleavage of recombinant Bcl-10 was evaluated by immunoblot analysis.

Adhesion assays. Central areas of tissue culture dishes (35-mm × 10-mm; 353001; BD Falcon) were coated for 90 min at 25 °C with 50 μl of fibronectin solution (40 μg/ml; Roche). Coated dishes were washed three times with PBS (without Ca^{2+} and Mg^{2+}) and were blocked for 2 h with 1% (wt/vol) BSA in PBS. Cells were washed with Hank's balanced-salt solution (Gibco) and were left unstimulated or were stimulated for 30 min at 37 °C with PMA (100 ng/ml) or for 15 or 30 min at 37 °C with $MnCl_2$ (1 mM), or for 5 min at 37 °C with a combination of anti–human CD3ε (10 μg/ml of OKT3; Apotech) and anti-CD28 (10 μg/ml of CD28.2; Immunotech), followed by cross-linking for 2 min with goat anti-mouse (5 μg/ml; Jackson Laboratories). Subsequently, cell suspensions were added to fibronectin-coated tissue culture dishes followed by incubation for additional 30 min at 37 °C. Nonadherent cells were removed by washing of the dishes three to five times with Hank's balanced-salt solution. Adherent cells were counted in six separate fields with a microscope with an ocular counting reticule.

Note: Supplementary information is available on the Nature Immunology website.

ACKNOWLEDGMENTS

We thank I. Gonzalez and D. Vercammen for discussions; S. Turcotte and L. Mury for technical assistance; V. Posevitz and P. Romero for culture reagents; A. Golks for technical advice on 'Anderson' gels; and F. Martinon and J. Tschopp for critically reading the manuscript. The plasmid pRDI_292 was a gift from R. Iggo (Swiss Institute for Experimental Cancer Research); Jurkat, Hut78 and Raji cells were gifts from O. Acuto (Pasteur Institute); phycoerythrin-labeled HLA-A*0201 peptide multimers were provided by P. Guillaume and I. Luescher (Ludwig Institute for Cancer Research); silencing vectors targeting the α- and β-subunit of IKK were provided by Y. Refaeli (National Jewish Medical and Research Center); and Jurkat cells deficient in IKKγ (NEMO) and their parental control cells were provided by A. Ting (Mount Sinai School of Medicine). Supported by the Swiss National Science Foundation (M.Th., N.F. and N.R.), the Swiss Cancer League (M.Th.), the Novartis Foundation (M.Th.), the Vontobel Stiftung (M.Th.), Studienstiftung des Deutschen Volkes (S.H.), the Faculty of Biology and Medicine of the University of Lausanne (S.H.) and the Swiss National Center of Competence in Research–Molecular Oncology (N.R.).

AUTHOR CONTRIBUTIONS

F.R. and S.H. designed, did and analyzed the key experiments; A.P.-F., M.Ta., R.M., O.G. and D.R. did experiments; M.G. provided technical assistance; E.M.I. and N.R. provided human antigen-specific CTLs; N.F. provided new reagents; M.Th. designed and organized the study and wrote the paper; and all authors discussed the results and commented on the manuscript.

Published online at http://www.nature.com/natureimmunology
Reprints and permissions information is available online at http://npg.nature.com/reprintsandpermissions

1. Rawlings, D.J., Sommer, K. & Moreno-Garcia, M.E. The CARMA1 signalosome links the signalling machinery of adaptive and innate immunity in lymphocytes. *Nat. Rev. Immunol.* **6**, 799–812 (2006).
2. Weil, R. & Israel, A. Deciphering the pathway from the TCR to NF-κB. *Cell Death Differ.* **13**, 826–833 (2006).
3. Thome, M. CARMA1, BCL-10 and MALT1 in lymphocyte development and activation. *Nat. Rev. Immunol.* **4**, 348–359 (2004).
4. Matsumoto, R. *et al.* Phosphorylation of CARMA1 plays a critical role in T cell receptor-mediated NF-κB activation. *Immunity* **23**, 575–585 (2005).
5. Sommer, K. *et al.* Phosphorylation of the CARMA1 linker controls NF-κB activation. *Immunity* **23**, 561–574 (2005).
6. McAllister-Lucas, L.M. *et al.* Bimp1, a MAGUK family member linking protein kinase C activation to Bcl-10-mediated NF-κB induction. *J. Biol. Chem.* **276**, 30589–30597 (2001).
7. Bertin, J. *et al.* CARD11 and CARD14 are novel caspase recruitment domain (CARD)/membrane-associated guanylate kinase (MAGUK) family members that interact with BCL-10 and activate NF-κB. *J. Biol. Chem.* **276**, 11877–11882 (2001).
8. Gaide, O. *et al.* Carma1, a CARD-containing binding partner of Bcl-10, induces Bcl-10 phosphorylation and NF-κB activation. *FEBS Lett.* **496**, 121–127 (2001).
9. Gaide, O. *et al.* CARMA1 is a critical lipid raft-associated regulator of TCR-induced NF-κ B activation. *Nat. Immunol.* **3**, 836–843 (2002).
10. Wang, D. *et al.* A requirement for CARMA1 in TCR-induced NF-κB activation. *Nat. Immunol.* **3**, 830–835 (2002).
11. Egawa, T. *et al.* Requirement for CARMA1 in antigen receptor-induced NF-κB activation and lymphocyte proliferation. *Curr. Biol.* **13**, 1252–1258 (2003).
12. Newton, K. & Dixit, V.M. Mice lacking the CARD of CARMA1 exhibit defective B lymphocyte development and impaired proliferation of their B and T lymphocytes. *Curr. Biol.* **13**, 1247–1251 (2003).
13. Che, T. *et al.* MALT1/paracaspase is a signaling component downstream of CARMA1 and mediates T cell receptor-induced NF-κB activation. *J. Biol. Chem.* **279**, 15870–15876 (2004).
14. Shinohara, H. *et al.* PKCβ regulates BCR-mediated IKK activation by facilitating the interaction between TAK1 and CARMA1. *J. Exp. Med.* **202**, 1423–1431 (2005).
15. Wegener, E. *et al.* Essential role for IκB kinase β in remodeling Carma1-Bcl-10-MALT1 complexes upon T cell activation. *Mol. Cell* **23**, 13–23 (2006).

16. Wegener, E. & Krappmann, D. CARD-Bcl-10-MALT1 signalosomes: missing link to NF-κB. *Sci. STKE* **2007**, pe21 (2007).
17. Sun, L., Deng, L., Ea, C.K., Xia, Z.P. & Chen, Z.J. The TRAF6 ubiquitin ligase and TAK1 kinase mediate IKK activation by BCL-10 and MALT1 in T lymphocytes. *Mol. Cell* **14**, 289–301 (2004).
18. Zhou, H. *et al.* Bcl-10 activates the NF-κB pathway through ubiquitination of NEMO. *Nature* **427**, 167–171 (2004).
19. Oeckinghaus, A. *et al.* MALT1 ubiquitination triggers NF-κB signaling upon T cell activation. *EMBO J.* **26**, 4634–4645 (2007).
20. Zhou, H., Du, M.Q. & Dixit, V.M. Constitutive NF-κB activation by the t(11;18)(q21;q21) product in MALT lymphoma is linked to deregulated ubiquitin ligase activity. *Cancer Cell* **7**, 425–431 (2005).
21. Lucas, P.C. *et al.* Bcl-10 and MALT1, independent targets of chromosomal translocation in malt lymphoma, cooperate in a novel NF-κB signaling pathway. *J. Biol. Chem.* **276**, 19012–19019 (2001).
22. Uren, A.G. *et al.* Identification of paracaspases and metacaspases: two ancient families of caspase-like proteins, one of which plays a key role in MALT lymphoma. *Mol. Cell* **6**, 961–967 (2000).
23. Snipas, S.J. *et al.* Characteristics of the caspase-like catalytic domain of human paracaspase. *Biol. Chem.* **385**, 1093–1098 (2004).
24. Vercammen, D. *et al.* Type II metacaspases Atmc4 and Atmc9 of *Arabidopsis* thaliana cleave substrates after arginine and lysine. *J. Biol. Chem.* **279**, 45329–45336 (2004).
25. Bozhkov, P.V. *et al.* Cysteine protease mcII-Pa executes programmed cell death during plant embryogenesis. *Proc. Natl. Acad. Sci. USA* **102**, 14463–14468 (2005).
26. Gonzalez, I.J., Desponds, C., Schaff, C., Mottram, J.C. & Fasel, N. *Leishmania major* metacaspase can replace yeast metacaspase in programmed cell death and has arginine-specific cysteine peptidase activity. *Int. J. Parasitol.* **37**, 161–172 (2007).
27. Anderson, N.L. & Anderson, N.G. Analytical techniques for cell fractions. XXII. Two-dimensional analysis of serum and tissue proteins: multiple gradient-slab gel electrophoresis. *Anal. Biochem.* **85**, 341–354 (1978).
28. Gross, O. *et al.* Card9 controls a non-TLR signalling pathway for innate anti-fungal immunity. *Nature* **442**, 651–656 (2006).
29. Rueda, D. *et al.* Bcl-10 controls TCR- and FcγR-induced actin polymerization. *J. Immunol.* **178**, 4373–4384 (2007).
30. Tanner, M.J., Hanel, W., Gaffen, S.L. & Lin, X. CARMA1 coiled-coil domain is involved in the oligomerization and subcellular localization of CARMA1, and is required for T cell receptor-induced NF-κ B activation. *J. Biol. Chem.* **282**, 17141–17147 (2007).
31. Lobry, C., Lopez, T., Israël, A. & Weil, R. Negative feed back loop in T cell activation through IκB kinase-induced phosphorylation and degradation of Bcl-10. *Proc. Natl. Acad. Sci. USA* **104**, 908–913 (2007).
32. Vercammen, D. *et al.* Serpin1 of *Arabidopsis thaliana* is a suicide inhibitor for metacaspase 9. *J. Mol. Biol.* **364**, 625–636 (2006).
33. Ferch, U. *et al.* MALT1 directs B cell receptor–induced canonical nuclear factor-κB signaling selectively to the c-Rel subunit. *Nat. Immunol.* **8**, 984–991 (2007).
34. Kane, L.P., Lin, J. & Weiss, A. It's all Rel-ative: NF-κB and CD28 costimulation of T cell activation. *Trends Immunol.* **23**, 413–420 (2002).
35. Rose, D.M., Cardarelli, P.M., Cobb, R.R. & Ginsberg, M.H. Soluble VCAM-1 binding to α_4 integrins is cell-type specific and activation dependent and is disrupted during apoptosis in T cells. *Blood* **95**, 602–609 (2000).
36. Sixt, M., Bauer, M., Lammermann, T. & Fassler, R. β1 integrins: zip codes and signaling relay for blood cells. *Curr. Opin. Cell Biol.* **18**, 482–490 (2006).
37. Dustin, M.L., Bivona, T.G. & Philips, M.R. Membranes as messengers in T cell adhesion signaling. *Nat. Immunol.* **5**, 363–372 (2004).
38. Sims, T.N. & Dustin, M.L. The immunological synapse: integrins take the stage. *Immunol. Rev.* **186**, 100–117 (2002).
39. Mobley, J.L., Ennis, E. & Shimizu, Y. Differential activation-dependent regulation of integrin function in cultured human T-leukemic cell lines. *Blood* **83**, 1039–1050 (1994).
40. Kinashi, T. Intracellular signalling controlling integrin activation in lymphocytes. *Nat. Rev. Immunol.* **5**, 546–559 (2005).
41. Chen, C. *et al.* High affinity very late antigen-4 subsets expressed on T cells are mandatory for spontaneous adhesion strengthening but not for rolling on VCAM-1 in shear flow. *J. Immunol.* **162**, 1084–1095 (1999).
42. Vercammen, D., Declercq, W., Vandenabeele, P. & Van Breusegem, F. Are metacaspases caspases? *J. Cell Biol.* **179**, 375–380 (2007).
43. Boatright, K.M. & Salvesen, G.S. Mechanisms of caspase activation. *Curr. Opin. Cell Biol.* **15**, 725–731 (2003).
44. Mittelbrunn, M. *et al.* VLA-4 integrin concentrates at the peripheral supramolecular activation complex of the immune synapse and drives T helper 1 responses. *Proc. Natl. Acad. Sci. USA* **101**, 11058–11063 (2004).
45. Ruland, J. *et al.* Bcl-10 is a positive regulator of antigen receptor-induced activation of NF-κB and neural tube closure. *Cell* **104**, 33–42 (2001).
46. Shapiro, V.S., Truitt, K.E., Imboden, J.B. & Weiss, A. CD28 mediates transcriptional upregulation of the interleukin-2 (IL-2) promoter through a composite element containing the CD28RE and NF-IL-2B AP-1 sites. *Mol. Cell. Biol.* **17**, 4051–4058 (1997).